MSUCL-246
August 1977

Search for Parity Mixing in the ^{93}Tc $17/2^-$ Isomer: Measurements of Internal Conversion Coefficients*

B.A. Brown, F.M. Bernthal, R.A. Warner and L.E. Young

Cyclotron Laboratory, Michigan State University
East Lansing, Michigan 48824

Abstract

The internal conversion coefficients were measured for several transitions in ^{93}Tc with an electron spectrometer and a Ge(Li) detector. The ^{92}Mo(α,p2n) reaction was used to study the decay of the isomeric τ = 15 μsec $\overline{17}/2^-$ level at 2185.3 keV as well as the decay of the prompt $17/2^+$ level at 2185.0 keV. The experimental K-shell conversion coefficients for the $\overline{17}/2^- \rightarrow 13/2^+$ and $17/2^+ \rightarrow 13/2^+$ transitions imply $\Gamma(E2, \overline{17}/2^- \rightarrow 13/2^+)/\Gamma(E2 + M2 + E3, \overline{17}/2^- \rightarrow 13/2^+) \leq 0.33$. The energy difference between the prompt and delayed γ transitions to the $13/2^+$ level was measured to be 0.32 ± 0.03 keV. These results imply $|\langle 17/2^+ | H_{pv} | 17/2^- \rangle| \leq 0.13$ eV for the matrix element of the parity violating Hamiltonian.

NUCLEAR REACTIONS ^{92}Mo(α,p2n), E = 43 MeV; measured pulsed beam electronic timing, I_{ce}, I_γ, E_γ; deduced α_K, γ-multipolarity, parity mixing. Enriched target, electron spectrometer, Si(Li) and Ge(Li) detectors

I. Introduction

In a previous study[1] of ^{93}Tc, an isomeric $\overline{17}/2^-$ level, $\tau \simeq 15$ sec, at 2185 keV was found to lie only about 0.4 keV above a prompt $17/2^+$ level. The notation $\overline{17}/2^-$ refers to the state with a possible mixed parity, $|\overline{17}/2^-> = |17/2^-> + \alpha\ |17/2^+>$. The $17/2^+$ level decays to the $13/2^+$ level and shell-model calculations[1] give an estimate of $\tau \simeq 30$ psec for its mean lifetime. Since the lifetimes of the $17/2^+$ and $17/2^-$ levels differ by a factor of 5×10^5, the $\overline{17}/2^- \rightarrow 13/2^+$ decay is extremely sensitive to a small mixing of the $17/2^+$ into the $17/2^-$ level which can originate from a parity-violating weak interaction component in the nuclear force[2]. In Ref. 1 a limit of $|<17/2^+ \mid H_{pv} \mid 17/2^-> \mid \leq 0.34$ eV was obtained for the matrix element of the parity- violating Hamiltonian. The $17/2^-$ isomeric decay scheme is shown in Fig. 1.

Many experiments have shown evidence for parity violation in nuclear transitions[2]. These experiments serve as a unique test for the predictions of various models of the weak interaction concerning the interaction of hadrons with hadrons. Of particular interest is the presence of neutral currents predicted by the Weinberg-Salam model[3]. Neutral current events in both leptonic and semileptonic processes have been observed but their presence in purely hadronic interactions is of fundamental importance to the theories. The purely hadronic neutral current interactions are expected to be most easily observed in the nucleon-nucleon interaction.

In order to unambiguously relate the parity violations observed in nuclear transitions to the strength of the parity-violating Hamiltonian operator, several conditions are necessary. First, it is important to have a reliable microscopic model of the states involved, and this condition is simplified if the effect is mostly due to the mixing

of two nearly degenerate levels. A good example of this is the J = 1/2 doublet in ^{19}F which has been studied by Adelberger et al.[4] Here the $1/2^-$ state and $1/2^+$ ground state are separated by 110 keV and the next J = 1/2 levels are several MeV higher; the energies of these states are well described in the shell model with $p_{1/2}\ d_{5/2} s_{1/2}$ configurations. ^{93}Tc is very similar in this regard. The J = 17/2 levels are separated by only about 0.4 keV and the energies are well described by the shell model with predominant configurations of $g^4_{9/2} p_{1/2}$ and $g^3_{9/2} p^2_{1/2}$ for $17/2^-$ and $17/2^+$, respectively.

In addition, the parity violating matrix element should be large and not dominated by cancellation effects due to nuclear structure. The parity violating Hamiltonian operator is expected to have a strength on the order of 1 eV.[2] The matrix element

$$|<^{19}\mathrm{F}\ 1/2^+ \mid H_{pv} \mid ^{19}\mathrm{F}\ 1/2^-> \mid = 1.5 \pm 0.8\ \mathrm{eV}$$

obtained from the ^{19}F γ-ray asymmetry experiments[4] is thus considered large. In contrast, the very small value of

$$|<^{180}\mathrm{Hf}\ 8^+ \mid H_{pv} \mid ^{180}\mathrm{Hf}\ 8^-> \mid = (1.2 \pm 0.2) \times 10^{-6}\ \mathrm{eV}$$

implied from the ^{180}Hf measurements[5] is an example of the large cancellation effects which can occur, in this case due to the $\Delta K = 8$ change in the intrinsic rotational wave functions.

In Sec. IV these disparate values for the matrix elements from ^{19}F and ^{180}Hf are shown to be closely scaled to the experimental electric dipole matrix elements between the same states. Using a typical E1 strength for the mass-90 region, this empirical scaling relation implies a parity violating matrix element on the order of 1.0 to 0.1 eV for ^{93}Tc. The H_{pv} matrix element may be

reduced in ^{93}Tc compared to ^{19}F because the $17/2^-$ differs from the $17/2^+$ configuration by a $\Delta j=4$ or 5 change in one orbital.

The scaling relation implies an H_{pv} matrix element in ^{93}Tc comparable to the upper limit of 0.34 eV. This implies that the E2 component in the $17/2^- \rightarrow 13/2^+$ transition may be quite large. In this work we report on a measurement of the internal conversion coefficient (ICC) for the 750 keV $17/2^- \rightarrow 13/2^+$ transition. The calculated K-shell conversion coefficients[6] α_K are 1.45×10^{-3}, 3.92×10^{-3} and 3.36×10^{-3} for the E2, M2 and E3 multipolarities, respectively. Hence a measurement of the ICC is obviously sensitive to the amount of E2 admixture, but the existence of an E2 component is unambiguously indicated only if

$$1.45 \times 10^{-3} \leq \alpha_K (\text{exp}) < 3.36 \times 10^{-3}.$$

In the present experiment we establish a new upper limit of

$$| < 17/2^+ | H_{pv} | 17/2^- > | \leq 0.13 \text{ eV}$$

based on the ICC measurements and a new determination of the $17/2^+ - 17/2^-$ energy splitting. The experimental technique is described in Sec. II and the results are presented in Sec. III. The H_{pv} matrix element is discussed in Sec. IV including the relation of the present results with the ^{19}F and ^{180}Hf experiments. The scaling relation between the H_{pv} and E1 matrix elements is also discussed in Sec. IV.

II Experimental Technique

The reaction ^{92}Mo(α,p2n)^{93}Tc at $E_\alpha = 43$ MeV was used. The reaction ^{94}Mo(p,2n) at $E_p = 25$ MeV was also

investigated but the transitions of interest were far more prominent in the (α,p2n) data. Ge(Li) γ-ray spectra and electron spectra from the MSU on-line conversion-electron spectrometer were accumulated independently and simultaneously for prompt and delayed time intervals measured with respect to pulses from the cyclotron beam pulsing system.

The electron spectrometer is depicted in Fig. 2. Electrons are transported from the target chamber through a set of helical anti-positron vanes by the field of a double-focussing solenoidal magnet. The electron energy spectrum is obtained from a Si(Li) detector placed at the focus. Transmission for momenta matching the field settings is about 6%, while the momentum bite at any given field setting is about 20% FWHM. The efficiency of the spectrometer was flattened over the region of interest, $\approx$ 500 - 1000 keV, by sweeping the magnet with a triangular wave-form with a period of about one minute.

The target was a 490 μg/cm^2 rolled Mo metal foil enriched to 94% ^{92}Mo backed with a layer of 200 μg/cm^2 C to stop the recoils. It was oriented at 45% with respect to the beam as shown in Fig. 2. The beam was pulsed with a repetition time of 110 μsec and with a time-on period of 11 μsec.

A simplified diagram of the electronics is shown in Fig. 3. Energy vs. time spectra were accumulated for the Si(Li) and Ge(Li) detectors in the form of two 64 x 256 arrays. The average time-dependent dead time was obtained from a pulser introduced into each spectrum. The final energy spectra were obtained by summing channels in the 64-channel time spectra corresponding to about 25-μsec intervals after making dead time corrections on a channel-by-channel basis.

The Ge(Li)/electron spectrometer system efficiency ratio was obtained from a thin ^{206}Bi source placed at the target position. ^{206}Bi has a strong isolated 715-keV K-conversion electron from the $2^+ \rightarrow 0^+$ transition in ^{206}Pb

(Ref. 7) which is close in energy to the 730-keV K-conversion electron from the $\overline{17/2}^- \rightarrow 13/2^+$ transition in ^{93}Tc. The ^{206}Pb $2^+ \rightarrow 0^+$ internal conversion coefficient was calculated assuming a pure E2 multipolarity using the code CATAR written by Pauli and Raff[6];

$$\alpha_K(^{206}\text{Pb } 2^+ \rightarrow 0^+) = 8.11 \times 10^{-3}.$$

The energy dependence of the electron spectrometer efficiency was obtained from the ^{206}Bi source using the electron intensities measured by Kanbe et al.[7] The energy dependence of the Ge(Li) detector efficiency was obtained from the ^{206}Bi source and a ^{166m}Ho source placed at the target position.

III. Results

The electron and γ-ray spectra are shown in Fig. 4. The electron spectra have been expanded and shifted relative to the γ-ray spectra so that the K-shell conversion electrons are in line with their respective γ-rays. The Tc K-shell binding energy is 21.0 keV. The spectra are shown for three time regions; the "prompt" region of the 11-μsec beam-on period, the 3-29 μsec delayed region in which the delayed ^{93}Tc lines are dominant, and the 29-68 μsec delayed region in which γ rays with longer half lives are dominant.

Peak areas were obtained by fitting with Gaussians which include exponential tails or, for isolated peaks, by summing counts above background. The relative efficiency curves were used to obtain intensities, and the final number for the internal conversion coefficient was obtained by normalizing to the 803-keV ^{206}Bi γ ray as discussed in Sec. II. The experimental K-shell internal conversion coefficients are given in Table 1 for a number of transitions in the region of interest around the ^{93}Tc 750-keV transition.

It was shown in Ref. 1 that the 750-keV γ ray was made up of a prompt $17/2^+ \rightarrow 13/2^+$ transition and a delayed $\overline{17/2}^- \rightarrow 13/2^+$ transition which were separated by about 0.4 keV. This is dramatically confirmed by the very different conversion coefficients obtained in and out of beam for this transition. The prompt internal conversion coefficient given in Table 1 for the 750-keV transition has been corrected for a 14.4% contribution of the delayed component in the 11-μsec in-beam period.

A weak 756-keV γ ray which originates from the ^{94}Ru $4^+ \rightarrow 2^+$ transition produced in the ^{92}Mo(α,2n) reaction appears in both the prompt and delayed periods. The peaks from K-shell electrons converted by the 750- and 756-keV transitions are not well resolved, so their areas were analyzed together, and a small correction for the 756-keV component was made in order to obtain the 750-keV conversion coefficients.

If there is any alignment of the nuclear states, corrections for the anisotropy of the γ rays and electrons should be included. The γ-ray angular distribution was measured for five angles between 0 and 90 degrees separately for the prompt and delayed events. In the delayed region the angular distributions were nearly isotropic. For example, the delayed 711-keV γ ray had an experimental angular distribution

$$W(\theta) = I_o[1 + A_2 P_2(\cos\theta) + A_4 P_4(\cos\theta)]$$

with $A_2 = -0.05 \pm 0.05$ and $A_4 = 0.04 \pm 0.07$ compared to the maximum alignment values[8] of $A_2 = 0.47$ and $A_4 = 0$ for a $13/2^- \rightarrow 13/2^+$ transition. The alignment loss is probably due to the time dependent quadrupole interactions from lattice defects caused by the recoiling atoms. Thus for the delayed transitions the angular distribution corrections are negligible since the γ's and e's are nearly isotropic.

The prompt $17/2^+ \rightarrow 13/2^+$ transition has an $A_2^\gamma \simeq 0.3$. The electron angular distributions are given by $A_k^e = b_k A_k^\gamma$ where the b_k are calculated[6,9] particle parameters; $b_2 = 1.40$ for the $17/2^+ \rightarrow 13/2^+$ transition. Taking into account the solid angles of the spectrometer and the Ge(Li) detector the angular distribution correction for the prompt $17/2^+ \rightarrow 13/2^+$ transition is estimated as only about ½% and hence has been neglected.

Finally, in the present experiment an energy difference of 0.32 ± 0.03 keV was measured between the prompt and delayed components of the 750-keV transition. This is three standard deviations lower than the result of 0.44 ± 0.02 keV obtained previously[1] with the $^{90}Zr(^6Li,3n)$ reaction. At present the best explanation for this discrepancy is that there is an unresolved weak contaminant γ ray that occurs in one of the reactions and not the other. The peak to background ratio is better in the present (α,p2n) experiment than it was in the (^{6}Li,3n) experiment. Thus, the present value of 0.32 ± 0.03 keV is adopted.

In the present experiment a limit of

$$BR(\overline{17}/2^- \rightarrow 17/2^+ \rightarrow 13/2^+) \,/\, BR(\overline{17}/2^- \rightarrow 13/2^+) \leq 0.1$$

for the ratio of the two branching ratios was obtained from an analysis of the delayed γ ray peak with two Gaussians. The measured energy shift between the prompt and delayed 750-keV transitions implies an energy difference of 0.32 ±0.03 keV between the $\overline{17}/2^-$ and $17/2^+$ states if there is no $\overline{17}/2^- \rightarrow 17/2^+ \rightarrow 13/2^+$ branch. The present limit on this branch implies an energy difference of

$$(0.32 \pm 0.03) \leq \Delta E \leq (0.35 \pm 0.03) \text{ keV}.$$

The internal conversion coefficient for a 0.32-keV E1 transition which involves the M4, M5... subshells was

calculated with the program CATAR[6] as 8.1×10^3. This, together with the lifetime and the present branching ratio limit, gives

$$B(E1, \overline{17}/2^- \rightarrow 17/2^+) \leq 4.1 \times 10^{-6} e^2 fm^2.$$

Typical E1 strengths for nuclei with 50 neutrons range from 10^{-4} to 10^{-6} e^2 fm^2 (see Table 4).

IV Discussion

The experimental and theoretical internal conversion coefficients are compared in Table 1. The transitions are divided into three groups; the ^{93}Tc prompt transition ($\tau \leq 1$ nsec), the ^{93}Tc delayed transitions ($\tau = 15$ μsec), and the ^{94}Mo delayed transitions which originate from the $T_{1/2} = 300$ min β decay of ^{94}Tc. The theoretical conversion coefficients were calculated with the program CATAR[6]. The CATAR values were in very good agreement with the values found by interpolating with tables of Hagar and Seltzer[10]. The experimental and theoretical agreement is excellent for the transitions which have predominantly E1 or E2 multipolarities.

For the ^{93}Tc $\overline{17}/2^- \rightarrow 13/2^+$ transition we obtain

$$\alpha_K \text{ (exp)} = (3.3 \pm 0.2) \times 10^{-3}$$

This is compared with the theoretical values assuming E2, M2 and E3 multipolarities in Table 2. Assuming at first no $\overline{17}/2^- \rightarrow 17/2^+ \rightarrow 13/2^+$ branch, α_K (exp) determines the following linear combination of the relative widths R for the $\overline{17}/2^- \rightarrow 13/2^+$ decay,

$$1.45\, R(E2) + 3.92\, R(M2) + 3.36\, R(E3) = 3.3 \pm 0.2$$

where, for example,

$$R(E2) = \Gamma(E2)/[\Gamma(E2) + \Gamma(M2) + \Gamma(E3)] .$$

A value for R(E2) cannot be determined until at least one other combination of the three multipolarities is known. Experiments to measure the mixing ratio $\delta(E3/M2)$ are currently being carried out[11]. In the two extremes $R(E2) = 0.25 \pm 0.08$ if $R(E3) = 0$ and $R(E2) = 0.03 \pm 0.10$ if $R(M2) = 0$. Thus without knowing $\delta(E3/M2)$ only a limit is obtained $R(E2) \leq 0.33$. This limit would be only slightly reduced if in addition the effect of a weak $17/2^- \rightarrow 17/2^+ \rightarrow 13/2^+$ branch is considered.

Following Ref. 1 the matrix element of H_{pv} is given by

$$|\langle 17/2^+ | H_{pv} | 17/2^- \rangle|$$

$$= \Delta E \left[\frac{\tau(17/2^+) \times BR(17/2^- \rightarrow 13/2^+) \times R(E2, 17/2^- \rightarrow 13/2^+)}{\tau(17/2^-)} \right]^{1/2}$$

where $\tau(17/2^-) = 15\ \mu sec$, $\tau(17/2^+) = 30$ psec (calculated in Ref. 1) and $BR(17/2^- \rightarrow 13/2^+) = 0.26$. Using the limit $R(E2, 17/2^- \rightarrow 13/2^+) \leq 0.33$ from the present experiment;

$$|\langle 17/2^+ | H_{pv} | 17/2^- \rangle| \leq 4.1 \times 10^{-4} \times \Delta E$$

Using a separation energy of $\Delta E = 0.32$ keV for the $17/2^+$ and $17/2^-$ levels we finally obtain

$$|\langle 17/2^+ | H_{pv} | 17/2^- \rangle| \leq 0.13 \text{ eV} .$$

This limit for ^{93}Tc is a factor of 10 times smaller than the value of

$$|\langle ^{19}\text{F}\ 1/2^+ | H_{pv} | ^{19}\text{F}\ 1/2^- \rangle| = 1.5 \pm 0.8 \text{ eV}$$

inferred from the experiments on ^{19}F (Ref. 4). However

the parity violating effects observed in ^{180}Hf (Ref. 5) imply the extremely small value

$$|\langle ^{180}\text{Hf}\ 8^+ | H_{pv} | ^{180}\text{Hf}\ 8^- \rangle| = (1.2 \pm 0.2) \times 10^{-6} \text{ eV}$$

Clearly, nuclear structure effects must be important.

It is interesting to compare the matrix element of the two-body operator H_{pv} to the matrix element of the one-body E1 operator which also connects the same levels. This is done in Table 3. For these few cases the matrix elements of the H_{pv} and E1 operators scale to a remarkable extent. This suggests that these two operators are sensitive to the nuclear structure in similar ways, which may imply for example that H_{pv} may be approximated by an effective one-body operator. Since the most important component of the E1 operator is of the isovector form $Y^{(1)} \tau$, one may speculate that also the most important part of the effective one-body parity violating operator is also an isovector, for example $[\sigma \times Y^{(1)}]^{(0)} \tau$. This would be interesting since it is the isovector $\Delta T = 1$ part of H_{pv} which is expected to be enhanced by the neutral currents[3].

The measured E1 and H_{pv} matrix elements in ^{93}Tc are consistent since they are both only upper limits. However, the upper limit on the E1 matrix element in ^{93}Tc is within the range of B(E1) values measured for transitions between levels which involve the $g_{9/2}p_{1/2}$ configurations in other N=50 nuclei as shown in Table 4. Thus, provided the actual E1 matrix element in ^{93}Tc is not anomalously small, the E1 scaling relation implies that $|\langle H_{pv} \rangle|$ should be on the order of 1.0 to 0.1 eV, which is consistent with the present upper limit of 0.13 eV

It will be interesting to pursue to the parity violating effects in ^{93}Tc. Further experiments on ^{93}Tc are being carried out[11] to measure the mixing ratio $\delta(E2/M2)$. γ-ray circular polarization and polarized beam experiments

could also be considered. Much needed theoretical calculations of the H_{pv} matrix elements based on the present models of the weak interaction should be carried out for ^{93}Tc. It would also be interesting to understand the scaling relation between the H_{pv} and E1 matrix elements on a theoretical basis.

*Research supported in part by the National Science Foundation.

[1]B.A. Brown, D.B. Fossan, P.M.S. Lesser and A.R. Poletti, Phys. Rev. C13, 1194(1976).

[2]M. Gari, Phys. Rep. C6, 319(1973); M.A. Box, B.H. McKeller, P. Pick and K.R. Lassey, J. Phys. G. 1, 439(1975).

[3]M. Gari in Interaction studies in Nuclei edited by A. Jochim and B. Ziegler (North-Holland, 1975) p. 307.

[4]E.G. Adelberger, H.E. Swanson, M.D. Cooper, J.W. Tape and T.A. Trainor, Phys. Rev. Lett. 34, 402(1975); E.G. Adelberger, H.E. Swanson and T.A. Trainor, Univ. of Seattle Annual Report 1976, p. 58.

[5]K.S. Krane, C.E. Olsen, J.R. Sites and W.A. Steyert, Phys. Rev. C4, 1906(1971); K.S. Krane, C.E. Olsen and W.A. Steyert, Phys. Rev. C5, 1663(1972).

[6]H.C. Pauli and U. Raff, Computer Physics Comm. 9, 392(1975).

[7]M. Kanbe, M. Fujioka and K. Hisatake, Nucl. Phys. A192, 151(1972).

[8]T. Yamazaki, Nucl. Data A3, 1(1967).

[9]W.D. Hamilton in The Electromagnetic Interaction in Nuclear Spectroscopy edited by W.D. Hamilton (North-Holland, 1975), p. 645.

[10]R.S. Hager and E.C. Seltzer, Nucl. Data A4, 1(1968).

[11]B.A. Brown, O. Hausser, T. Faestermann, D. Ward, H.R. Andrews and D. Horn, to be published.

[12]B.A. Brown, P.M.S. Lesser, and D.B. Fossan, Phys. Rev. C13, 1900(1976).

[13]D.C. Kocher, Nuclear Data Sheets 16, 55(1975).

[14]S. Cochavi, J.M. McDonald and D.B. Fossan, Phys. Rev. C3, 1352(1971).

TABLE 1. Experimental and theoretical internal conversion coefficients

E_γ (keV)	Assignment	α_K (exp) $\times 10^3$	Multi-polarity	α_K (th)[a] $\times 10^3$	α_K (exp)/α_K(th)
	^{93}Tc Prompt				
750.5	$17/2^+ \rightarrow 13/2^+$	1.40 ± 0.06	E2	1.45	0.96 ± 0.04
	^{93}Tc Delayed				
629.4	$13/2^- \rightarrow 11/2^+$	0.93 ± 0.08	E1	0.82	1.13 ± 0.10
711.1	$13/2^- \rightarrow 13/2^+$	0.66 ± 0.05	E1	0.63	1.05 ± 0.08
750.8	$\overline{17}/2^- \rightarrow 13/2^+$	3.3 ± 0.2	b	b	
	^{94}Mo Delayed				
702.4	$4^+ \rightarrow 2^+$	1.65 ± 0.03	E2	1.61	1.02 ± 0.02
847.7	$6^+ \rightarrow 4^+$	0.98 ± 0.02	E2	1.00	0.98 ± 0.02

a Calculated with CATAR (Ref. 6)
b See Table 2

TABLE 2. K-Shell internal conversion coefficient for the isomeric 750.8 keV transition in ^{93}Tc

α_K (exp)	Multipolarity	α_K (th)[a]
$(3.3 \pm 0.2) \times 10^{-3}$	E2	1.450×10^{-3}
	M2	3.921×10^{-3}
	E3	3.363×10^{-3}

a Calculated with CATAR (Ref. 6).

TABLE 3. Comparison of experimental E1 strengths and matrix elements of the parity violating Hamiltonian $|\langle H_{pv} \rangle|$ deduced from various experiments.

Nucleus	J	Ref.	ΔE (keV)	B(E1) ($e^2fm^2 \times 10^{-6}$)	$[B(E1)]^{1/2}$ (e fm $\times 10^{-2}$)	$\lvert \langle H_{pv} \rangle \rvert$ (eV)
^{19}F	1/2	a	110	560 ± 12	2.4	1.5 ± 0.8
^{93}Tc	17/2	b	0.32	$\leq$ 4.1	$\leq$ 0.20	$\leq$ 0.13
^{180}Hf	8	c	57	0.78 $\times 10^{-6}$	0.88 $\times 10^{-6}$	(1.2 ± 0.2) $\times 10^{-6}$

a Ref. 4
b Present experiment
c Ref. 5

TABLE 4 Experimental E1 strengths for nuclei with 50 neutrons.

Nucleus	$J_i \rightarrow J_f$	B(E1) ($e^2fm^2 \times 10^{-6}$)	$[B(E1)]^{1/2}$ (e fm $\times 10^{-2}$)	Refs.
^{90}Zr	$6^+ \rightarrow 5^-$	34[a]	0.58	b
^{91}Nb	$17/2^+ \rightarrow 17/2^-$	≤ 3.7[a]	≤ 0.19	c
	$17/2^+ \rightarrow 19/2^-$	57[a]	0.75	c
^{92}Mo	$5^- \rightarrow 4^+$	19.3 ± 0.5	0.44 ± 0.01	d
	$6^+ \rightarrow 5^-$	67 ± 7	0.82 ± 0.04	d
^{93}Tc	$17/2^+ \rightarrow 17/2^-$	≤ 4.1	≤ 0.20	e

a Based on calculated mean lifetimes of $\tau = 12.7$ psec for the ^{90}Zr 6^+ state and 10.9 psec for the ^{91}Nb $17/2^+$ state obtained from the experimental branching ratio of the $6^+ \rightarrow 4^+$ and $17/2^+ \rightarrow 13/2^+$ transitions, respectively, together with theoretical B(E2) values (Ref. 12).
b Ref. 13
c Ref. 12
d Ref. 14
e Present experiment

FIG. 1. Decay scheme for the ^{93}Tc $17/2^-$ isomer from the present work and Ref. 1. The dashed lines indicate transitions for which only an upper limit on their strengths have been established.

FIG. 2. Horizontal cross section through the axis of the electron spectrometer showing the detector in counting position.

FIG. 3. Simplified diagram of electronics used to accumulate 2-parameter spectra (energy vs. time) for both electrons and γ-rays. The pulse generator is used for dead-time corrections.

FIG. 4. Comparison of γ-ray and electron spectra from the ^{92}Mo(α,p2n) reaction at E_α=43 MeV. Three time regions are shown, an in-beam spectrum and two delayed time regions. The transitions discussed in the text are labeled. The electron spectra have been shifted and expanded so that the peaks appear under the appropriate γ-rays.

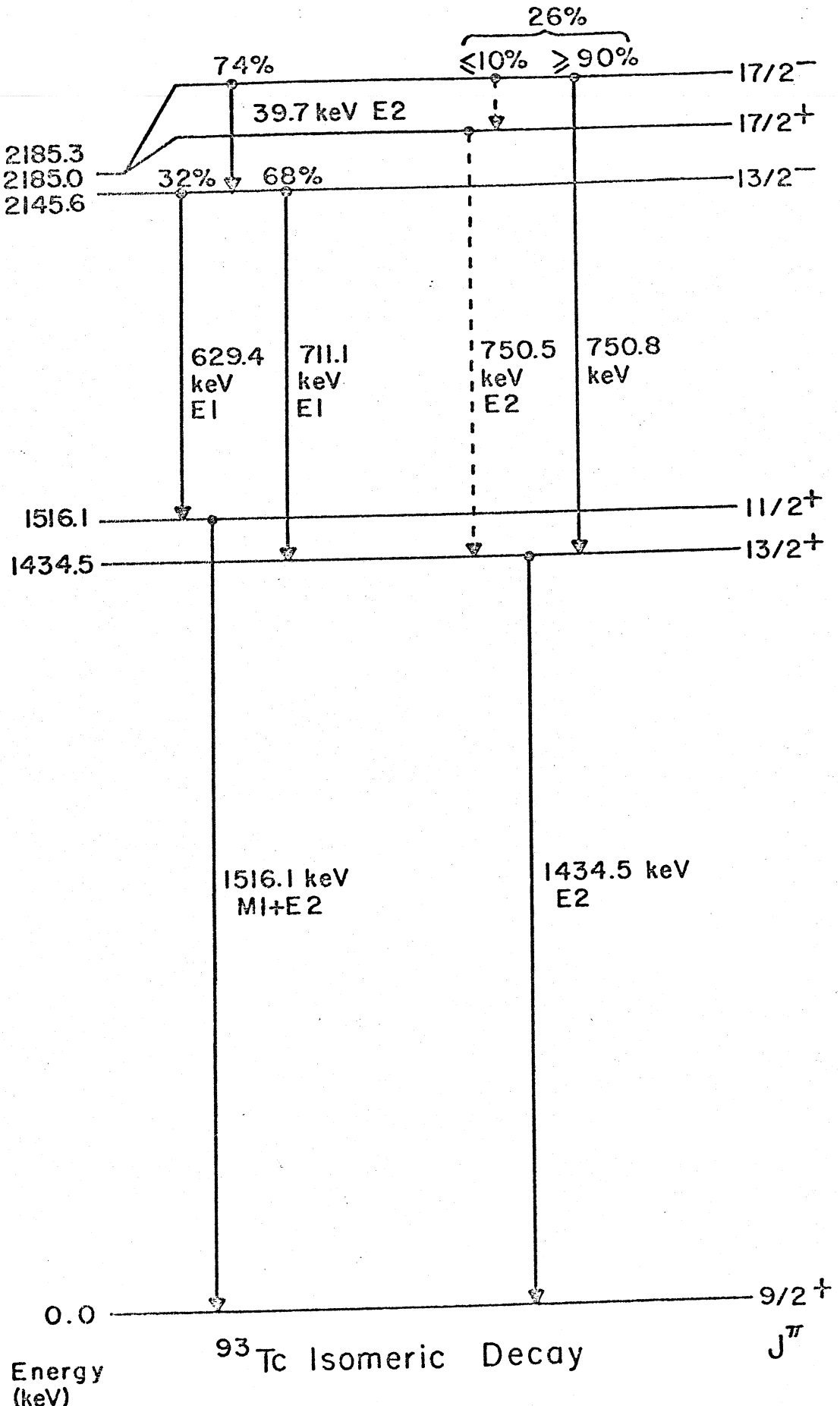
26%
74%
≤10%
≥90%
17/2⁻
39.7 keV E2
17/2⁺
2185.3
2185.0
2145.6
32%
68%
13/2⁻
629.4 keV E1
711.1 keV E1
750.5 keV E2
750.8 keV
1516.1
11/2⁺
1434.5
13/2⁺
1516.1 keV M1+E2
1434.5 keV E2
0.0
9/2⁺
Energy (keV)
93Tc Isomeric Decay
Jπ

Fig. 1

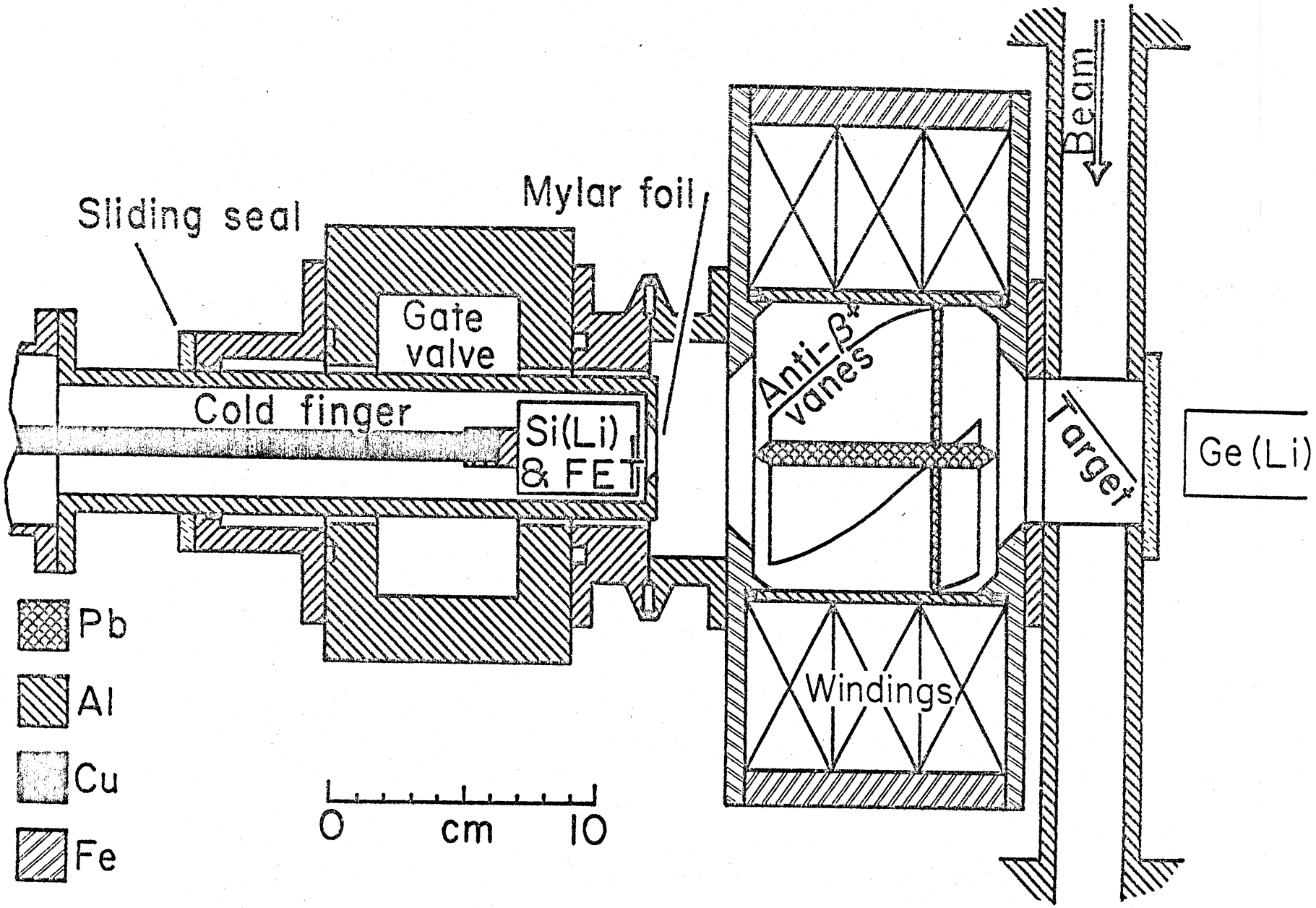
Sliding seal
Mylar foil
Beam
Gate valve
Anti-β⁺ vanes
Cold finger
Si(Li) & FET
Target
Ge(Li)
Pb
Al
Cu
Fe
Windings
0
cm
10

Fig. 2

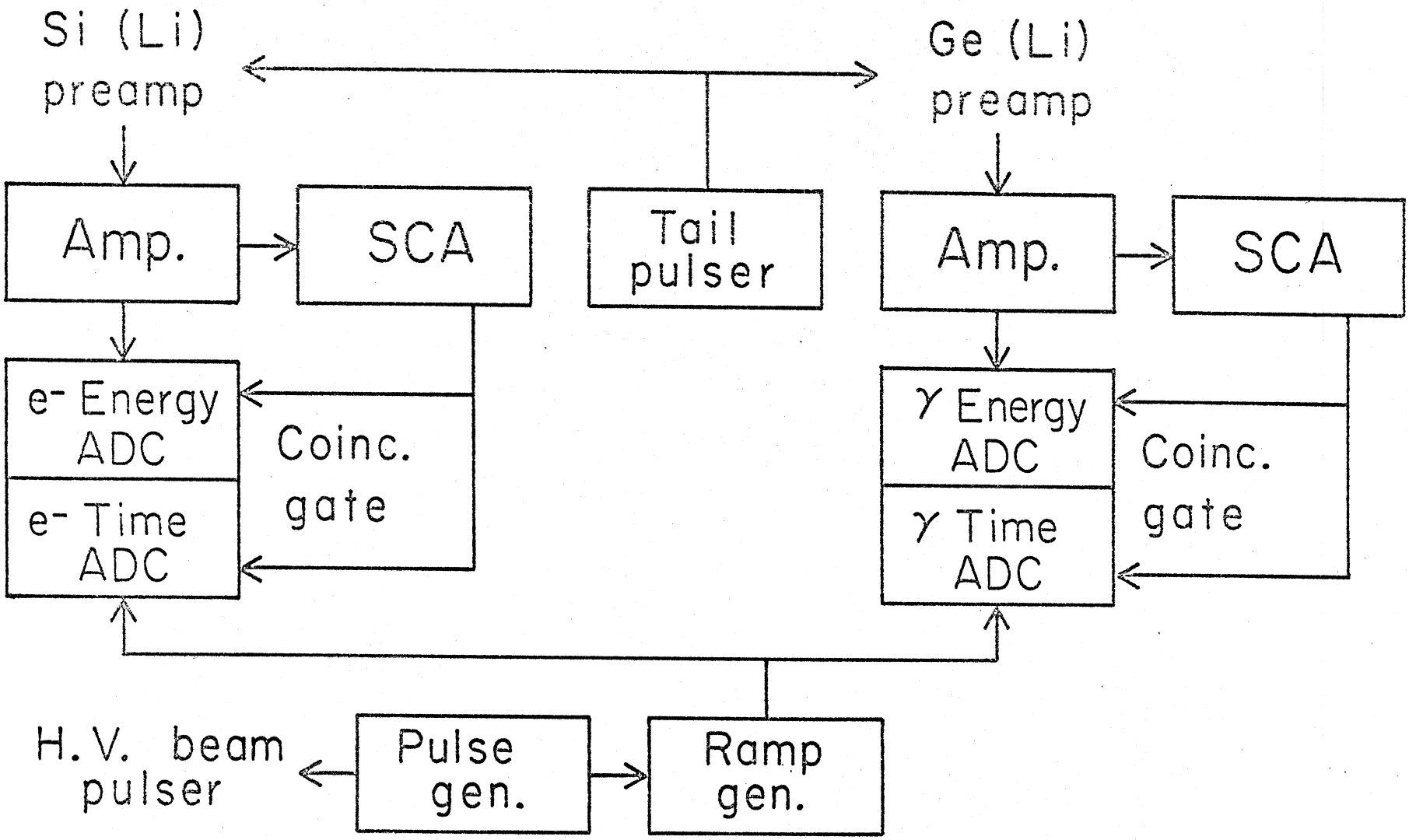
Si (Li)
preamp
Ge (Li)
preamp
Amp.
SCA
Tail
pulser
Amp.
SCA
e⁻ Energy
ADC
e⁻ Time
ADC
Coinc.
gate
γ Energy
ADC
γ Time
ADC
Coinc.
gate
H.V. beam
pulser
Pulse
gen.
Ramp
gen.

Fig. 3

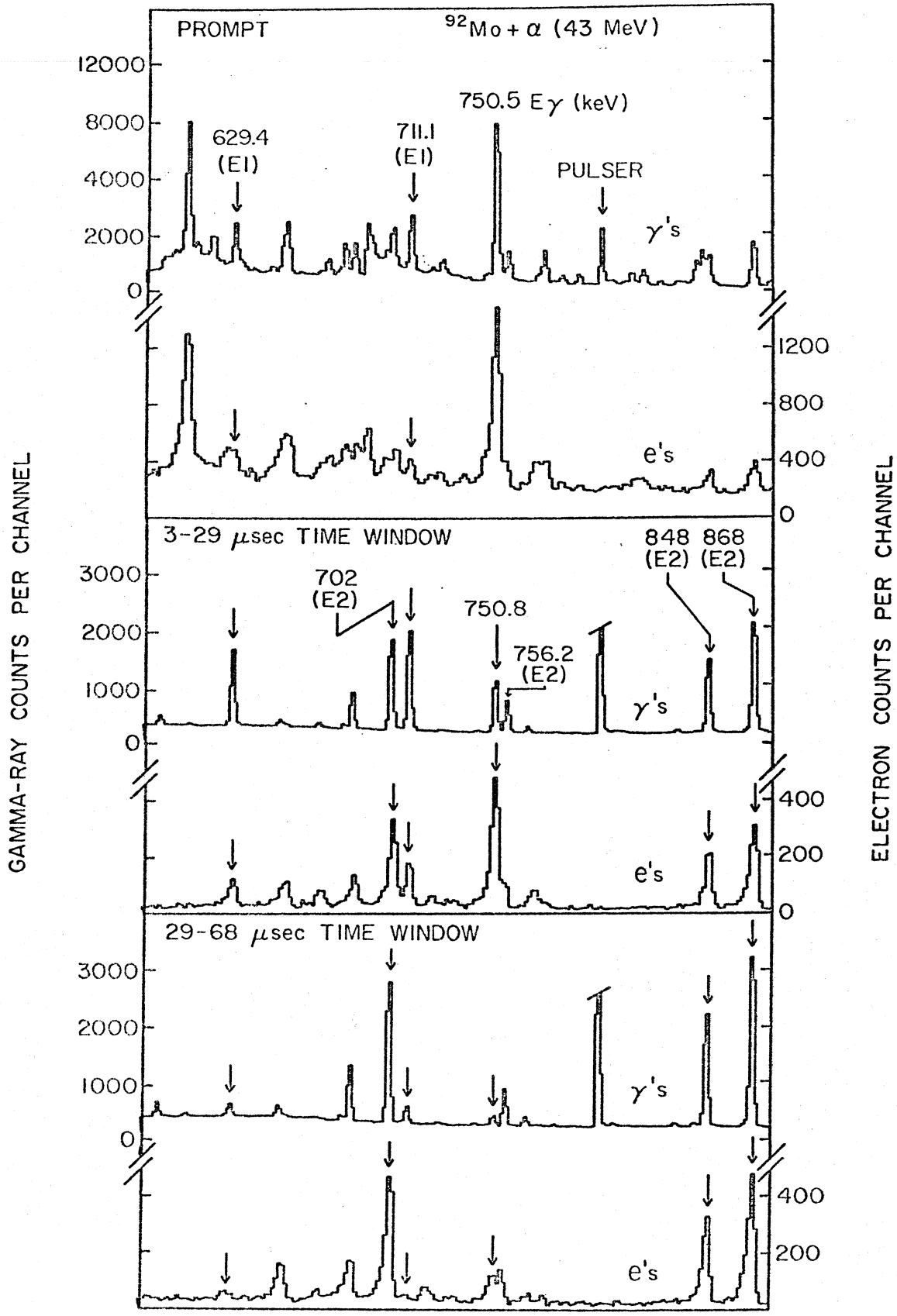

CHANNELS 15-256 FOR GAMMA RAYS
CHANNELS 23-220 FOR ELECTRONS

Fig. 4